



A comparison of total precipitable water measurements from radiosonde and sunphotometers

Elies Campmany^{a,*}, Joan Bech^{a,b}, Javier Rodríguez-Marcos^{a,c}, Yolanda Sola^a, Jerónimo Lorente^a

^a Dept. Astronomia i Meteorologia, Universitat de Barcelona, Martí i Franquès 1, Barcelona 08028, Spain

^b Servei Meteorològic de Catalunya, Berlin 38-48 4a, Barcelona 08029, Spain

^c Agencia Estatal de Meteorología (AEMET), Paseo del Canal 17, Zaragoza 50007, Spain

ARTICLE INFO

Article history:

Received 2 June 2009

Received in revised form 23 April 2010

Accepted 29 April 2010

Keywords:

Total precipitable water

Radiosonde

Sunphotometer

Cimel

Microtops

ABSTRACT

Atmospheric water vapour is an essential component of the terrestrial atmosphere and must be known precisely in a wide range of applications such as radiative transfer modelling or weather forecasting to mention just a few examples. Vertically integrated measurements, or total precipitable water (TPW) equivalent amounts traditionally derived from radiosonde measurements, are needed in many of these applications and can also be obtained from other methodologies such as sunphotometers or GPS-based techniques. This paper presents a study comparing different measurements of TPW from radiosonde and sunphotometer data recorded from 2001 to 2004 in Barcelona, Spain. Three collocated instruments were employed in this study: RS-80A Vaisala sondes and two types of commonly used sunphotometers (Cimel 318N-VBS7 and Microtops II). A cloud screening filter was applied to photometer data based on the quality control procedure of the AERONET database.

A systematic comparison among the measurements indicates that bivariate correlations between different instruments were high, with correlation factors (r^2) above 0.8 in all cases. Measurements covered all seasons allowing examining intra-annual variability, which generally did not exhibit statistically significant differences. Examination of 57 concurrent measurements of the three instruments indicated that radiosonde TPW measurements were the highest (15 mm on average) and Cimel and Microtops presented similar values (12 mm and 11 mm respectively).

© 2010 Elsevier B.V. All rights reserved.

1. Introduction

The knowledge of accurate values of water vapour present in the atmosphere is essential for the monitoring and forecasting tasks of most meteorological processes. The horizontal and vertical distributions of water vapour are also important factors for understanding the hydrological cycle variations and climate change and global warming studies, as water vapour is the most abundant greenhouse gas.

During decades the traditional instrument used to measure the water vapour vertical profile has been the radiosonde. However, this has some limitations, such as imprecision in the estimation of moisture due to different causes like the freezing of moisture sensors, the release of latent heat, the phase lag between dry and wet bulb sensors. Measurements of moisture profile from radiosondes allow estimating the total precipitable water (TPW), i.e., the integrated amount of water vapour in the vertical column from the ground to the top of the atmosphere,

$$TPW = \frac{1}{g} \sum_{i=1}^n q_i \Delta p_i \quad (1)$$

where g is the acceleration due to gravity, n is the number of atmospheric layers considered and q_i is the mean specific humidity corresponding to atmospheric layer i with a pressure

* Corresponding author. Present address: Earth Sciences Dept., Barcelona Supercomputing Center, Jordi Girona 29, Barcelona 08034, Spain. Tel.: +34 934134038.

E-mail address: elies.campmany@bsc.es (E. Campmany).

increment Δp_i . TPW, also known as water (vertical) column abundance, is normally expressed in kg m^{-2} (or its equivalent depth in mm if all water vapour in the column was condensed). The specific humidity is not a direct measurement of the radiosonde but can be written in terms of the dew point temperature.

When a global distribution of water vapour is considered, the radiosonde measurements are generally insufficient because of their irregular and poor spatial and temporal coverage. Other type of water vapour measurements, like those based on satellite observations, including retrievals from Global Positioning System (GPS) measurement, or ground based radiometers can complement radiosonde derived TPW observations (Stoew et al., 2001; Dostalek and Schmit, 2001; Chaâbane et al., 2006; Martinez et al., 2007).

Because of its simplicity and its lower cost TPW can be obtained from sunphotometers when direct sunlight reaches the ground. They are simple to use and offer a higher spatial and temporal resolution than radiosounding data, but less coverage than from satellite measurements. Since the use of these instruments requires cloudless conditions at least in front of the sun, sunphotometers measurements are biased toward cloud-free conditions. The uncertainty of TPW from sunphotometers is mainly due to some aging effects in the filters incorporated in these instruments, which can be analyzed by comparison (Plana-Fattori et al., 1998).

Comparisons between TPW values obtained from radiosondes and sunphotometers have been carried out in different places. For example, Halthore et al. (1997) made a comparison between Cimel sunphotometer and radiosonde data with simultaneous measurements during clear-sky conditions (July 1993) at Wallops Island, Virginia (US). The results showed differences of 10% in TPW between radiosonde and sunphotometer data (the latter with lower values). The same authors made a comparison between the same instruments in the Atmospheric Radiation Measurement (ARM) project (Oklahoma, US) in April 1994 and obtained that the sunphotometer overestimated the TPW derived from radiosonde by about 9.2%. Revercomb et al. (2003) reported differences up to 15% between radiosonde and MicroWave Radiometer (MWR) with the radiosonde typically being drier than the MWR in a 2-year comparison of measurements conducted at the ARM site in Oklahoma between 1996 and 2000.

The main objective of this paper is the comparison of TPW values obtained simultaneously during the period 2001–2004 over the same point of observation from the radiosonde and two kind of sunphotometers currently employed in the solar measurement networks, the Microtops II and Cimel instruments. In addition, a preliminary climatology of the TPW during this period is presented.

2. Data

2.1. Radiosonde

Since 1997, radiosonde observations have been made at the Astronomy and Meteorology Department of the University of Barcelona (41°23' N, 2°7' E and 98 m above sea level) to support the operations of the regional administration's Subdirectorate of Air Quality and Meteorology. Observations are performed operationally twice a day at 00 and 12 UTC (00

and 12 LST) using Vaisala RS-80A sondes. Measurements, recorded every 10 s., include temperature, pressure, relative humidity and wind speed and direction.

As radiosonde data are available for relative long time series, they are the traditional source for upper-air climatological studies, for example devoted to characterise humidity conditions (Elliott and Gaffen, 1991) or temperature (Luers and Eskridge, 1995; Zhai and Eskridge, 1996). However, some potential instrumental problems and environmental factors may affect the quality and representativeness of measurements, particularly, but not only, in the lowest layers of the troposphere (Parlange and Brutsaert, 1990; Connel and Miller, 1995; Free et al., 2002). For example, recent efforts to build global re-analysis data sets have considered different methods to correct radiosonde systematic temperature bias, including satellite observations such as the NOAA Vertical Profile Radiometer (Andrae et al., 2004; Li et al., 2005).

According to Bruegge et al. (1992) total water vapour estimated with radiosonde measurements presents three main sources of error: (a) overestimate of moisture after freezing and subsequent latent heat release (which may introduce up to 8% errors); (b) different time lags between dry and wet bulb temperature measurements (up to 6% errors); and (c) higher atmospheric layers not sampled by radiosonde ascents (up to 8% errors). Other authors, as Miloshevich et al. (2006), suggest a maximum of 6–8% dry bias daytime measurements due to the solar heating of the sensor. In our data set, the correction suggested in that study yielded differences mostly <1% so this was finally not applied.

2.2. Sunphotometer Microtops II

The Microtops II v.2.4X is a multi-band sunphotometer capable of measuring the total ozone column, the TPW and the aerosol optical thickness at 1020 nm (Morys et al., 2001). The instrument is equipped with 5 optical collimators with a full field of view (FOV) of 2.5°. Each channel is fitted with an interference filter and a photodiode that produces an electrical current proportional to the measured power. The instrument measures the direct beam of the solar irradiance in the wavelengths of 305.5, 312.5, 320.0, 936.0 and 1020.0 nm with a full width at half maximum (FWHM) of 2 ± 0.3 nm for the 3 channels of the UV region and a FWHM of 10 ± 1 nm for the other two.

The instrument is calibrated with Langley plots from Mauna Loa (Hawaii, 3397 m a.s.l.) recorded under different meteorological conditions. The retrieval of the TPW is based on measurements taken at 936 nm (water absorption peak) and 1020 nm (no water absorption). Because of the nonlinear dependence of the atmospheric transmission on TPW, the response voltage V_{936} of the sunphotometer is given by the Modified Beer Law (Reagan et al., 1987; Bruegge et al., 1992):

$$\ln V_{936} + m\tau_{\text{scat}} = \ln V_0 - a(wm)^b \quad (2)$$

where τ_{scat} is the sum of the Rayleigh and aerosol optical depths (τ_a) contributions in the 936-nm channel, m is the air mass and w is the total precipitable water (TPW). The parameters a and b are adjustable constants depending on the instrument characteristics (i.e. the bandwidth of the filter) and the atmospheric conditions (i.e., pressure, temperature and

vertical distribution of water vapour). These constants are generally determined using a radiative transfer model (Halthore et al., 1997; Alexandrov et al., 2009). The values of both constants are introduced in the instrument by the manufacturer ($a=0.7847$ and $b=0.5945$).

The determination of the TPW requires the aerosol optical depth contribution at 936 nm. This value is not calculated by the instrument but it is derived from the aerosol optical depth at 1020 nm, internally computed following the Beer's law. From a radiative transfer model, a relationship between the aerosol optical depths at both wavelengths is found for a standard atmosphere and it is assumed constant for other conditions. For the Microtops filters the relationship is $\tau_{a936} = 1.16\tau_{a1020}$ (Morys et al., 2001).

2.3. Sunphotometer Cimel

The Cimel 318N-VBS7 is a motor-tracked sunphotometer which points automatically to the Sun (Cimel, 2001). This instrument is the standard Sun/sky photometer from the AEROSOL ROBOTIC NETWORK (AERONET) (Holben et al., 1998). It has an optical header with two collimators (a glassless one to observe the Sun and another with glasses to observe the sky). The whole FOV is 1.2° . This header points to the Sun using two microprocessors that calculate the zenithal and azimuthal angle from the geographical coordinates and the date and time. The orientation is finally sharpened with a four-quadrant detector with a precision of 0.1° . The instrument has 7 channels 340, 380, 440, 675, 870, 936 and 1020 nm with a FWHM of 10 nm (except for the channels of 340 and 380 nm which have a FWHM of 2 nm). Cimel instrument measures the direct irradiance, the almucantar irradiance (i.e., observed along a circle parallel to the horizon at a given elevation angle) and the principal plane irradiance (over an arc of varying elevation angle given a fix azimuth) at the Earth's surface. For each measurement the instrument covers all 7 filters in 8 s and after a break of 20 s, it repeats the series two times more; therefore for either channel there are 3 non-simultaneous measurements available. The direct sun triplets are used to perform cloud discrimination and stability controls following the AERONET standard algorithm (Smirnov et al., 2000).

The Cimel instrument was calibrated by the Langley technique using the most stable days of the data set with air masses varying from 2 to 6. For the 936-nm filter, the calibration was determined using the “modified Langley plot,” taking logarithms at both sides of Eq. (2). As it was explained for the Microtops algorithm description, the pair of constants a and b are numerically derived based on the modelled spectral irradiances at 936 nm. Halthore et al. (1997), using the MODTRAN-3 radiative transfer (RT) model, determined a and b for the Cimel CE318 filters. In this work we have used these constants differing between summer ($a=0.616$, $b=0.593$) and winter ($a=0.616$, $b=0.597$).

Schmid et al. (2001) showed that the use of a single RT model produces a spread of 0.22 cm (8%) in TPW among different types of solar radiometers. In the same way, Alexandrov et al. (2009) presented a detailed analysis of the errors in TPW retrieval due to uncertainties in the calibration, in the instrument filter profiles and water vapour absorption line parameters in HITRAN spectral database. The estimated uncertainties in multifilter rotating shadowband radiometer (MFRSR) associated with calibration, spectral response filter (SRF) and spectral databases were 4.5%, 4.4% and 5%, respectively for solar noon in summer.

3. Results and discussion

Fig. 1 shows the TPW retrieved using radiosonde, Microtops and Cimel sunphotometer. The radiosonde data is the longest and most continuous series of the three instruments and includes 3.5 years of data. TPW has a seasonal behaviour with a maximum in summer and a minimum in winter. This is due to the fact that a higher air temperature implies a larger capacity to store water vapour without saturation. Maximum values reach 42 mm and minimum values around 2 mm. The range between the maximum and the minimum values for the same season is approximately constant, around 25 mm.

The TPW measured by the sunphotometer Microtops is more discontinuous than the previous one because the instrument needs cloud-free conditions, at least between the sun and the sunphotometer, to discern the solar disk (DeFelice and Wylie, 2001). However, the period of the series is long enough

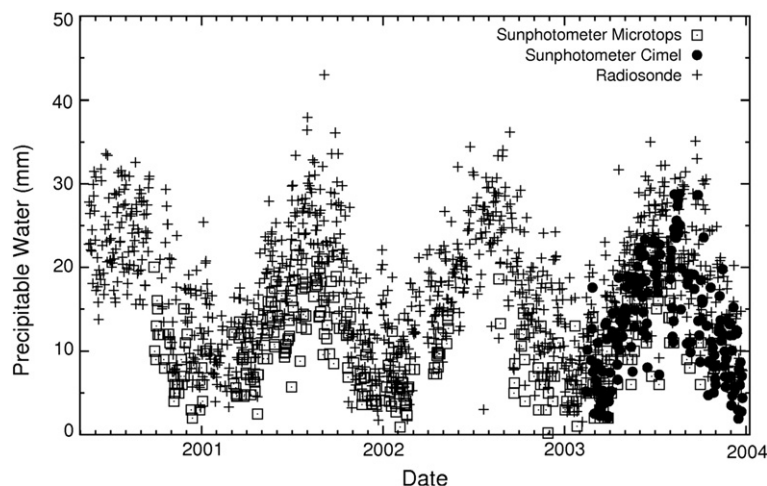


Fig. 1. Comparison between total precipitable water retrieved by radiosonde, Microtops and Cimel data recorded in Barcelona.

to appreciate the same seasonal behaviour deduced in the first series. In this case, the maximum value reaches 22 mm and the minimum is almost 0. The range is not as constant as in the radiosonde data and is approximately equal to 10 mm. There is a gap in the summer of 2002 because the instrument was used in a field campaign in Southern Spain (Alados-Arboledas et al., 2003; Sola et al., 2008).

The TPW retrieved from the Cimel data corresponds to 2003 (the instrument was installed in January of the same year). Although the instrument performs several measurements during daytime, only the value closer to midday is plotted to ensure maximum simultaneity with the other measurements. A cloud screening filter has been applied using the quality control of the AERONET database (Smirnov et al., 2000). The same seasonal pattern noticed in the radiosonde and the Microtops sunphotometer is present in this series. In this case the maximum value reaches 35 mm and the minimum is almost 0 mm. Data range is roughly constant as well, approximately 15 mm.

Intra-annual range is quite regular, approximately 15 mm. Most of the upper points correspond to radiosonde data, while in the lower part of the graph there is a greater amount of Microtops data. This can be explained by the fact that radiosonde data shown in Fig. 1 include cloudy days with typically higher values of TPW.

Table 1 shows the temporal period covered, the total number of data available, and the average and standard deviation of TPW retrieved with each instrument. In the case of Cimel photometer, only one measurement per day has been considered. The number of concurrent or simultaneous measurements available for the three instruments is relatively small in comparison with the total number of data available for each single instrument. The mean for the radiosonde and Cimel data is substantially lower in the simultaneous measurements than considering the whole data sets. This can be explained considering that a coincident measurement is always in a sunny period (with less water vapour content in the atmosphere than in a cloudy day) since the Microtops photometer only performs measurements under cloudless conditions. No attempt was made to study TPW temporal trends as the time series were too limited for that purpose.

The time of the radiosonde measurements is local noon (launch time). Although a radiosonde takes about one hour and a half to acquire all the data, the boundary layer, where most water vapour is present, is sampled just after launch. At launch time (12 UTC) a manual Microtops sunphotometer measurement was carried out at the same place of the launching. In

Table 1

Period covered, number of data available, average and standard deviation of total precipitable water retrievals for each single instrument (radiosonde and Microtops and Cimel sunphotometers) and for simultaneous measurements (last row).

	Radiosonde	Microtops	Cimel
Period	May2000– Dec2003	Sep2000– Nov2003	Feb2003– Dec2003
Number of data	1225	490	184
Mean \pm std dev (mm)	17 \pm 8	10 \pm 5	13 \pm 7
Mean \pm std dev (mm) for simultaneous measurements (57)	15 \pm 7	11 \pm 5	12 \pm 7

the case of the Cimel sunphotometer, which operates automatically at the same launching site, the measurement closer to 12 UTC has been considered.

No cloud screening filter was applied to the radiosonde data. Fig. 1, which shows 12 UTC values, exhibits a rather continuous plot. On the contrary, sunphotometer data are more discontinuous due to the fact that in that case only clear-sky observations are available.

In order to quantify and evaluate the differences among the three instruments, linear fits between pairs of them have been calculated (Fig. 2). Fig. 2a shows the least square line fit between Microtops and radiosonde data. The radiosonde retrievals have higher values than the Microtops-derived water vapour estimations. However it can be appreciated that both retrievals are strongly correlated. Fig. 2b shows the linear fit between Cimel and radiosonde data. In this case the slope is almost equal to 1, which indicates a very good agreement

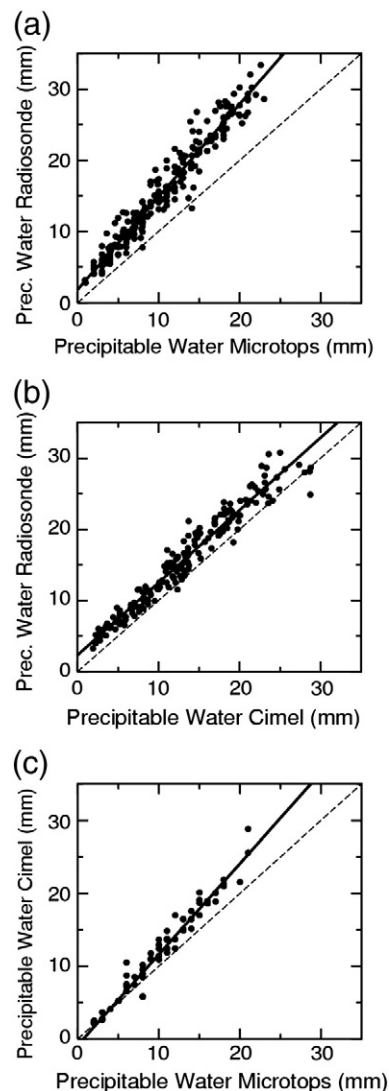


Fig. 2. Least squares linear fits between water vapour retrievals obtained with the following datasets: (a) Microtops–Radiosonde; (b) Cimel–Radiosonde; and (c) Microtops–Cimel.

Table 2

Least squares linear fit $y = ax + b$, between total precipitable water retrieved from radiosonde and two sunphotometers (Microtops and Cimel) data.

	Microtops (x)– Radiosonde (y)	Microtops (x)–Cimel (y)	Cimel (x)– Radiosonde (y)
<i>a</i>	1.30 ± 0.02	1.25 ± 0.03	1.02 ± 0.02
<i>b</i>	1.8 ± 0.2	−0.8 ± 0.4	2.3 ± 0.3
<i>r</i> ²	0.945	0.943	0.947
N. points	235	78	180

between both retrievals. Since the radiosonde also gives higher values of TPW it produces the highest water vapour estimates of the 3 instruments.

Finally, Fig. 2c exhibits the linear fit between the 2 sunphotometers. Though it is the fit with less number of points, it can be appreciated that both variables are well correlated. However, Microtops values are lower than Cimel TPW with the deviation increasing as the TPW increases. This behaviour is probably due to the value of the *a* constant (Eq. (2)) set by the manufacturer ($a = 0.7847$) which might be inexact. Ichoku et al. (2002) determined a new empirically-derived *a* value of 0.615 that is very close to the constant determined for the Cimel filter by Halthore et al. (1997) and used in this work. With the new *a* value and new calibration coefficients, Ichoku et al. (2002) found an improvement in RMSE between Cimel and Microtops TPW-derived (<0.1 cm). Another source of inaccuracy is the way the internal Microtops algorithm determines τ_{a936} as $1.12\tau_{a1020}$, assuming this relationship is always constant.

The water vapour retrieved by Cimel is higher than the one measured by Microtops such as in the Microtops–radiosonde comparison, hence Microtops measurements provide the lowest water vapour estimations of the 3 instruments. Table 2 shows the coefficients of the 3 least square line fits

Table 3

Mean Bias Error (MBE) and Root Mean Square Error (RMSE) of relative and absolute differences among the 3 total precipitable water retrievals: Microtops–Radiosonde, Microtops–Cimel and Cimel–Radiosonde.

	Absolute differences		Relative differences	
	MBE [mm]	RMSE [mm]	MBE [%]	RMSE [%]
Microtops–Radiosonde	−5.37	3.76	−35.32	21.94
Microtops–Cimel	1.97	1.71	17.41	14.84
Cimel–Radiosonde	−2.62	1.76	−18.97	12.29

and their correlation. The best fit is for the comparison between Cimel and radiosonde (Fig. 2b) which obtains a correlation factor of 0.947.

Fig. 3 shows the relative and absolute differences between couples of the 3 instruments. It is remarkable that the differences between Microtops and radiosonde retrievals have the highest values in both relative and absolute terms. In this case, the differences are mainly negative, which confirm the results shown in Fig. 2a. However, there are some positive values that are considerably high, especially in the relative differences plot. The maximum value for the absolute differences is around 20 mm and for the relative ones around 75%. These great differences between Microtops and radiosonde retrievals have been reflected in the BIAS and the RMSE shown in Table 3, which are the highest for the 3 comparisons.

Considering the differences between Microtops and Cimel, these are mainly positive in concordance with Fig. 2c. In this case the differences have lower values (the maximum relative difference is around 50% and the absolute is 5 mm) and the BIAS and the RMSE show a better agreement as well.

Finally, the difference between Cimel and radiosonde is mainly negative as could be expected from Fig. 2b, and it can be appreciated a lower relative difference in summer, since

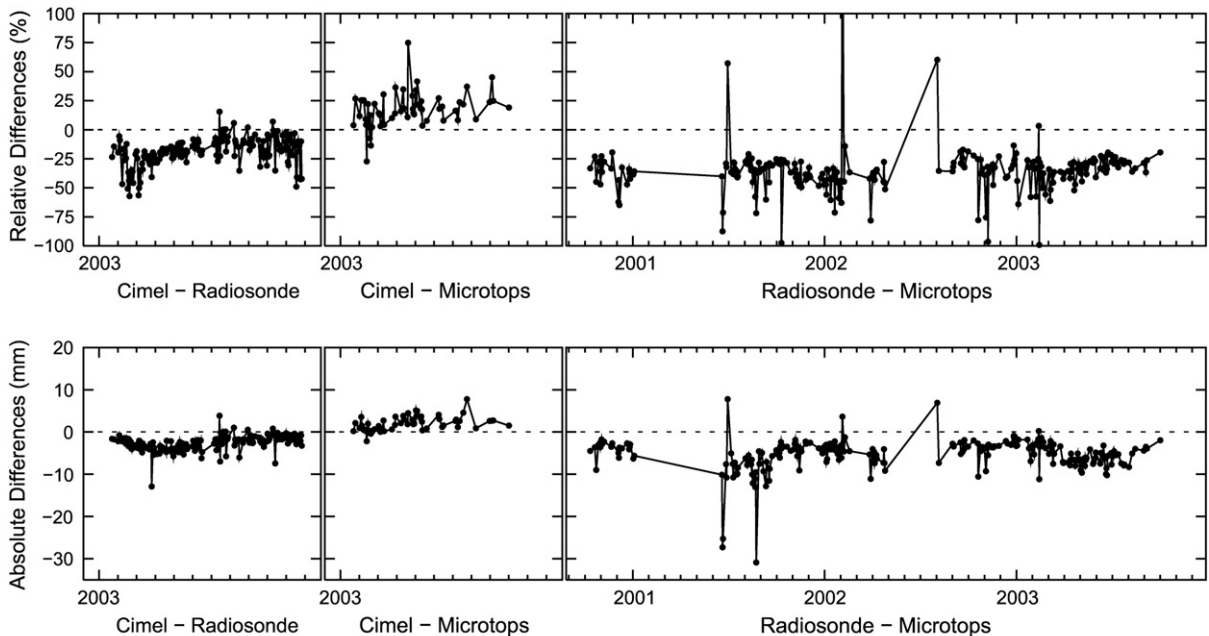


Fig. 3. Time series of absolute and relative differences among Radiosonde, Microtops and Cimel data recorded in Barcelona.

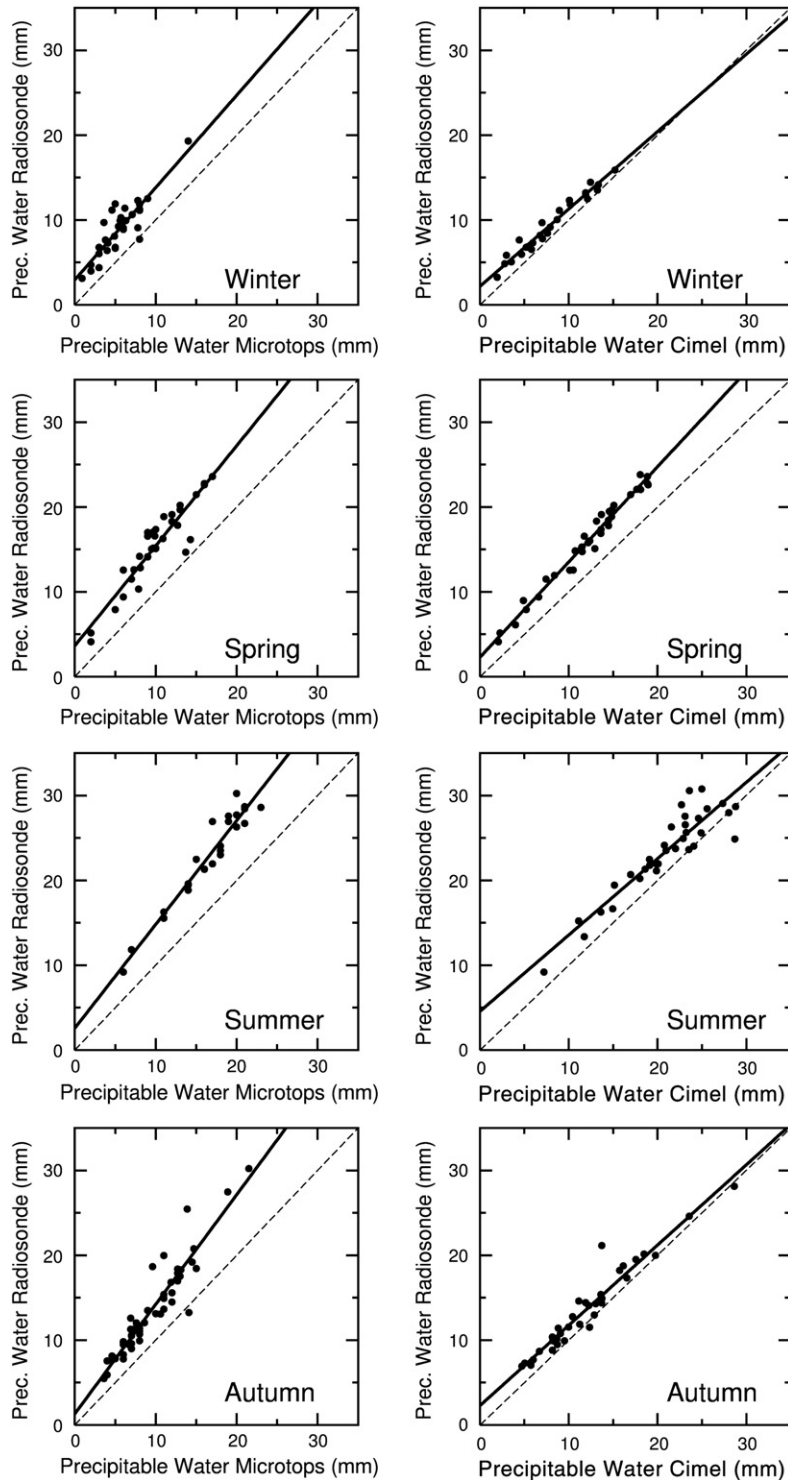


Fig. 4. Least squares linear fits between Radiosonde and the sunphotometers water vapour retrievals for different seasons: winter (December and February), spring (April and May), summer (July and August) and autumn (October and November).

the value of the TPW in the denominator is greater. The maximum of these differences is around 50% for the relative ones and for the absolute ones around 10 mm. However the BIAS and the RMSE show good agreement. RMSE of these

relative differences (shown in Table 3) exhibits a value of 12.29%, close to the 10% proposed by Halthore et al. (1997) in the comparison between Cimel and radiosonde data at Wallops Island, mentioned above.

Table 4

Least squares linear fit $y = ax + b$, between total precipitable water retrieved by radiosonde and by two sunphotometers (Microtops and Cimel).

Instrument	Season	a	b	r^2	# points
Microtops (x)– Radiosonde (y)	Winter	1.10 ± 0.10	2.9 ± 0.7	0.83	31
	Spring	1.18 ± 0.08	3.6 ± 0.9	0.89	34
	Summer	1.22 ± 0.07	2.0 ± 1.0	0.94	24
	Autumn	1.29 ± 0.07	1.3 ± 0.7	0.85	50
Cimel (x)– Radiosonde (y)	Winter	0.91 ± 0.04	2.2 ± 0.3	0.83	26
	Spring	1.10 ± 0.03	2.3 ± 0.4	0.87	34
	Summer	0.90 ± 0.07	5.0 ± 1.0	0.94	35
	Autumn	0.94 ± 0.05	2.3 ± 0.6	0.85	34

Fig. 4 and Table 4 show the correlations between radiosonde data and the sunphotometers for different seasons (December and February for winter, April and May for spring, July and August for summer and October and November for autumn). The seasonal behaviour mentioned before is also present especially in the winter plot where all the points have low values, and in the summer plot with higher values. Table 4 shows that the value of the slope and correlations change slightly with the season. In case of the Microtops and radiosonde comparison, the slope oscillates between 1.10 (winter) and 1.29 (autumn) while in the case of the Cimel and radiosonde comparison the oscillation is between 0.90 (summer) and 1.10 (spring). The variations in the correlations only vary significantly (with a confidence level $p = 0.05$) between Cimel and radiosonde data during summer and winter and summer and autumn; the rest of variations are not significant.

4. Summary and conclusions

Total precipitable water measurements from radiosonde and two different sunphotometers (Cimel and Microtops instruments) have been carried out and compared in Barcelona, Spain. The length of the time series examined spanned from 3.5 years (radiosonde data) to 11 months (Cimel sunphotometer); 57 simultaneous measurements for the three instruments were available in cloudless conditions and a higher number was used for comparison between two instruments. Results show a similar seasonal pattern of the three time series with a maximum in summer, a minimum in winter and an intra-annual range about 15 mm. The radiosonde data show generally higher TPW values (on average 15 mm for the simultaneous measurements), and a better agreement with the Cimel sunphotometer. The finding of higher values of TPW measured by radiosondes compared to photometers is qualitatively in agreement with previous studies, as that by Halthore et al. (1997) performed at Wallops Island (US), though there are some differences in the methodology of both studies which hampers a detailed comparison.

The two time series of the sunphotometers are well correlated, but average TPW values from Cimel are slightly higher (12 mm) than those corresponding to Microtops II (11 mm); the RMSE between the TPW of the photometers is <2 mm. In most cases the correlations between instruments did not change substantially in different seasons – i.e. with higher or lower TPW values. This is an interesting result considering that in other studies comparing several instruments measuring TPW – for example that of Liou et al. (2001) using radiosondes

and GPS-based techniques near the Tropics – a dependence on the amount of TPW of the differences between instruments was found.

As the period examined is relatively short to study possible TPW trends, this aspect was not considered in this research. However, other studies with larger datasets generally indicate increasing TPW amounts. For example, a variation of a little less than 1% per year was found over Boulder (US) over a 14-year period (AGU, 1995), in agreement with Ross and Elliott (1996) who found an increase of 3–7% per decade of TPW for trends south of 45°N in North America. Ross and Elliott (2001) and Trenberth et al. (2005) found later similar results for the whole Northern Hemisphere. The study of possible TPW trends in Barcelona is therefore left for future research when longer time series will be available for further analysis.

Acknowledgment

This work was supported by the Spanish Ministry of Science and Technology under the project DAMOCLES ‘Aerosols characterization by columnar (lidar and extinction) and “in situ” measurements’ (REF: CGL2005-03428-C04-04).

References

- AGU, 1995. Water Vapor in the Climate System. AGU Special Report. American Geophysical Union, 2000 Florida Ave., N.W., Washington, DC 20009.
- Alados-Arboledas, L., et al., 2003. VELETA 2002 field campaign. Geophys. Res. Abst. 5, 12,218.
- Alexandrov, M.D., Schmid, B., Turner, D.D., Cairns, B., Oinas, V., Laci, A.A., Gutman, S.I., Westwater, E.R., Smirnov, A., Eilers, J., 2009. Columnar water vapor retrievals from multifilter rotating shadowband radiometer data. J. Geophys. Res. 114, D02306. doi:10.1029/2008JD010543.
- Andrae, U., Sokka, N., Onogi, K., 2004. The radiosonde temperature bias corrections used in ERA-40. ERA-40 Project Report Series 15. European Centre for Medium-Range Weather Forecasts, 34 pp.
- Bruegge, C.J., Conel, J.E., Green, R.O., Margolis, J.S., Holm, R.G., 1992. Water vapor column abundance retrievals during FIFE. J. Geophys. Res. 97 (D17), 18,759–18,769.
- Chaâbane, M., Masmoudi, M., Medhioub, K., Elleuch, F., 2006. Daily and monthly averaged aerosol optical properties and diurnal variability deduced from AERONET sun-photometric measurements at Thala site (Tunisia). Meteorol. Atmos. Phys. 92, 103–114.
- Cimel, 2001. Sunphotometer User Manual Cimel CE 318, V. 4.6. Cimel. 172 rue de Charonne, 75011 Paris, France, 79 pp.
- Connel, B.H., Miller, D.R., 1995. Interpretation of radiosonde errors in the atmospheric boundary layer. J. Appl. Meteor. 34, 1070–1081.
- DeFelice, T.P., Wylie, B.K., 2001. Sky type discrimination using a ground-based sun photometer. Atmos. Res. 59–60, 313–329.
- Dostalek, J.F., Schmit, T.J., 2001. Total precipitable water measurements from GOES sounder derived product imagery. Wea. Forecast. 16, 573–587.
- Elliott, W.P., Gaffen, D.J., 1991. On the utility of radiosonde humidity archives for climate studies. Bull. Amer. Meteor. Soc. 72, 1507–1520.
- Free, M., et al., 2002. Creating climate reference datasets: CARDS workshop on adjusting radiosonde temperature data for climate monitoring. Bull. Amer. Meteor. Soc. 83, 891–899.
- Halthore, R.N., Eck, T.F., Holben, B.N., Markham, B.L., 1997. Sun photometric measurements of atmospheric water vapor column abundance in the 940-nm band. J. Geophys. Res. 102 (D4), 4343–4352.
- Holben, B.N., et al., 1998. AERONET – a federated instrument network and data archive for aerosol characterization. Remote Sens. Environ. 106 (D11), 12,067–12,097.
- Ichoku, C., Levy, R., Kaufman, Y.J., Remer, L.A., Li, R.-R., Martins, V.J., Holben, B.N., Abuhassan, N., Slutsker, I., Eck, T.F., Pietras, C., 2002. Analysis of the performance characteristics of the five-channel Microtops II Sun photometer for measuring aerosol optical thickness and precipitable water vapor. J. Geophys. Res. 107 (D3), 4179. doi:10.1029/2001JD001302.

- Li, X., Kelly, G., Uppala, S., Saunders, R., Gibson, J.K., 2005. The use of VTPR raw radiances in ERA-40. ERA-40 Project Report Series 21. European Centre for Medium-Range Weather Forecasts. 20 pp.
- Liou, Y.A., Teng, Y.T., Van Hove, T., Liljegren, J.C., 2001. Comparison of precipitable water observations in the near tropics by GPS, microwave radiometer, and radiosondes. *J. Appl. Meteorol.* 40, 5–15.
- Luers, J.K., Eskridge, R.E., 1995. Temperature correction for the VIZ and Vaisala radiosondes. *J. Appl. Meteorol.* 34, 1241–1253.
- Martinez, M.A., Velazquez, M., Manso, M., Mas, I., 2007. Application of LPW and SAI SAFNWC/MSG satellite products in pre-convective environments. *Atmos. Res.* 83, 366–379.
- Miloshevich, L.M., Vomel, H., Whiteman, D.N., Lesht, B.M., Schmidlin, F.J., Russo, F., 2006. Absolute accuracy of water vapor measurements from six operational radiosonde types launched during AWEX-G and implications for AIRS validation. *J. Geophys. Res.* 111, D09S10. doi:10.1029/2005JD006083.
- Morys, M., Mims III, F.M., Hagerup, S., Anderson, S.E., Baker, A., Kia, J., Walkup, T., 2001. Design, calibration, and performance of MICROTOS II handheld ozone monitor and Sun photometer. *J. Geophys. Res.* 106 (D13), 14,573–14,582.
- Parlange, M.B., Brutsaert, W., 1990. Are radiosonde time scales appropriate to characterize boundary layer wind profiles? *J. Appl. Meteorol.* 29, 249–255.
- Plana-Fattori, A., Legrand, M., Tanré, D., Devaux, C., Vermeulen, A., 1998. Estimating the atmospheric water vapor content from sun photometer measurements. *J. Appl. Meteorol.* 37 (8), 790–804.
- Reagan, J.A., Thome, K., Herman, B., Gall, R., 1987. Water vapor measurements in the 0.94 micron absorption band – calibration, measurements and data applications. IGARSS '87. International Geoscience and Remote Sensing Symposium, Ann Arbor, MI, May 18–21, 1987. : Digest, Volume 1 (A87-53101 24-43). Institute of Electrical and Electronics Engineers, New York, pp. 63–67.
- Revercomb, H.E., Turner, D.D., Tobin, D.C., Knuteson, R.O., Feltz, W.F., Barnard, J., Bösenberg, J., Clough, S., Cook, D., Ferrare, R., Goldsmith, J., Gutman, S., Halthore, R., Lesht, B., Liljegren, J., Linné, H., Michalsky, J., Morris, V., Porch, W., Richardson, S., Schmid, B., Splitt, M., Van Hove, T., Westwater, E., Whiteman, D., 2003. The ARM program's water vapor intensive observation periods, overview, initial accomplishments, and future challenges. *Bull. Am. Meteorol. Soc.* 84, 217–236.
- Ross, R.J., Elliott, W.P., 1996. Tropospheric water vapor climatology and trends over North America: 1973–93. *J. Climate* 9, 3561–3574.
- Ross, R.J., Elliott, W.P., 2001. Radiosonde-based Northern Hemisphere tropospheric water vapor trends. *J. Climate* 14, 1602–1612.
- Schmid, B., Michalsky, J.J., Slater, D.W., Barnard, J.C., Halthore, R.N., Liljegren, J.C., Holben, B.N., Eck, T.F., Livingston, J.M., Russell, P.B., Ingold, T., Slutsker, I., 2001. Comparison of columnar water-vapor measurements from solar transmittance method. *Appl. Opt.* 40 (12), 1889–1896.
- Smirnov, A., Holben, B.N., Eck, T.F., Dubovik, O., Slutsker, I., 2000. Cloud screening and quality control algorithms for the AERONET database. *Remote Sens. Environ.* 73, 337–349.
- Sola, Y., et al., 2008. Altitude effect in UV radiation during the evaluation of the effects of elevation and aerosols on the ultraviolet radiation 2002 (VELETA-2002) field campaign. *J. Geophys. Res.* 113, D23202. doi:10.1029/2007JD009742.
- Stoew, B., Elgered, G., Johansson, J.M., 2001. An assessment of estimates of integrated water vapor from ground-based GPS data. *Meteorol. Atmos. Phys.* 77, 99–107.
- Trenberth, K.E., Fasullo, J., Smith, L., 2005. Trends and variability in column-integrated atmospheric water vapor. *Clim. Dyn.* 24, 741–758.
- Zhai, P., Eskridge, R., 1996. Analyses of inhomogeneities in radiosonde temperature and humidity time series. *J. Climate* 9, 884–896.